

# Pulse-Bias Electronics and Techniques for a Josephson Arbitrary Waveform Synthesizer

Samuel P. Benz, *Fellow, IEEE*, and Steven B. Waltman, *Member, IEEE*

**Abstract**—The Josephson arbitrary waveform synthesizer (JAWS) is a series array of thousands of superconducting Josephson junctions that are biased by current pulses such that the array produces voltage waveforms with quantum accuracy. Intrinsically accurate voltage waveforms synthesized with the quantized pulses from Josephson junctions were first demonstrated in 1996. Ten years later, a commercial ac standard was calibrated at an output root-mean-square (RMS) amplitude of 100 mV with the first practical superconducting digital-to-analog converter. Since then, many different bias techniques, pulse-drive electronics, and device technology have been developed and improved in order to achieve a maximum of 138 mV output RMS voltage per Josephson array. In this paper, we report new bias electronics and demonstrate two new pulse-bias techniques. The first technique has demonstrated 250 mV output RMS voltage per 6400-junction array and may enable a practical 1 V system with only four arrays. The second bias technique reduces inductance-related error signals at the signal frequency and should reduce systematic errors for waveforms with frequencies greater than 1 MHz.

**Index Terms**—Digital-analog conversion, Josephson arrays, quantization, signal synthesis, standards, superconducting integrated circuits, voltage measurement.

## I. INTRODUCTION

**D**ESPITE nearly two decades of development, Josephson arbitrary waveform synthesizer (JAWS) systems have not yet achieved an output RMS voltage of 1 V. A single pulse-driven Josephson junction behaves like a perfect digital-to-analog converter (DAC) that produces accurate and undistorted waveforms because precisely one perfectly quantized output pulse is produced for every input bias pulse [1], [4]–[6], which we call the “ $n = 1$ ” quantum state. Series arrays of thousands of junctions are required to increase the output voltage to practical values because of the very small  $\sim 2 \mu\text{V}/\text{GHz}$  frequency-to-voltage conversion factor that is defined by the flux quantum  $h/2e$ , where  $h$  is Planck’s constant, and  $e$  is the electron charge [7]–[10]. Because the synthesized voltage waveforms are intrinsically accurate and distortion free, pulse-driven arrays and their associated bias electronics have been developed for ac voltage standards, and the ac voltage standards, in turn, have

Manuscript received May 28, 2014; revised June 19, 2014 and June 30, 2014; accepted June 30, 2014. Date of publication July 11, 2014; date of current version November 17, 2014. This paper was presented in part in presentation 4EB-06, “Bipolar ternary-coded pulse-bias technique for voltage waveform synthesis,” at the 2012 Applied Superconductivity Conference, Portland, Oregon, USA, October 11, 2012. This paper was recommended by Associate Editor O. Mukhanov.

S. P. Benz is with the National Institute of Standards and Technology, Boulder, CO 80305 USA (e-mail: benz@nist.gov).

S. B. Waltman is with the National Institute of Standards and Technology, Boulder, CO 80305 USA, and also with High Speed Circuit Consultants, Boulder, CO 80302 USA (e-mail: steve@hsccl.biz).

Digital Object Identifier 10.1109/TASC.2014.2338326

been used to characterize high-performance analog and digital electronics [11]–[27].

The maximum output RMS voltage of a circuit with two series arrays of 6400 Josephson junctions, operating in the  $n = 1$  state, is currently 275 mV [3]. The circuits and systems have been referred to as either AC Josephson Voltage Standards (ACJVS) when used for voltage calibrations or JAWSs when the emphasis is on the generation of distortion-free multitone waveforms. One JAWS version called a quantized voltage noise source generates a comb of equal-amplitude random-phase harmonics to produce a pseudonoise waveform that is used to calibrate low-noise amplifier chains in electronic primary temperature standards based on Johnson noise thermometry [13], [24]. The ACJVS systems, in particular, are designed to generate dc and low-frequency ( $< 1$  MHz) sine-wave voltages in order to calibrate ac voltage detectors such as thermal converters and transfer standards.

## II. WAVEFORM SYNTHESIS WITH QUANTIZED PULSES

The original demonstration [1] of the Josephson DAC used a digital pulse generator to produce programmable unipolar dc voltages, in which the resulting time-averaged voltage was determined by the density of pulses. The first advance in bias techniques, which achieved a sixfold improvement in voltage over unipolar synthesis, enabled bipolar waveforms to be synthesized [4], [5]. Bipolar pulses were produced by combining a two-level digital code (typically provided by an Agilent 70843A pattern generator)<sup>1</sup> with a microwave signal of frequency  $f_m$  (typically 15 GHz) that is an odd half-integer multiple ( $f_m = (m/2) f_s$ , where  $m = 1, 3, 5, \dots$  and typically  $m = 3$ ) of the digital signal’s non-return-to-zero (NRZ) clock frequency  $f_s$  (typically 10 GHz). The second advance [12] was to “ac-couple” the digital bias, which removed unwanted common-mode signals on the termination resistors and thereby enabled series connection of two arrays, doubling the combined output voltage. Other advances such as cryopackaging [28], stacked junctions [29], [30], new materials for Josephson junction barriers [31]–[33], bias lead filters [34], and tapered transmission lines [35] also contributed to increasing the RMS voltage per array to 138 mV.

Fig. 1 shows the simplified schematic for the ac-coupled “bipolar” bias technique for a single array [4], [5], [12]. Two high-speed biases, i.e., the digital bit code data (D) clocked at

<sup>1</sup>Commercial instruments are identified in this paper in order to adequately specify the experimental procedure. Such identification does not imply recommendation or endorsement by the National Institute of Standards and Technology nor does it imply that the equipment identified are necessarily the best available for the purpose.

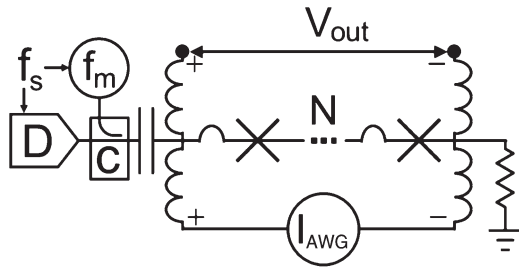


Fig. 1. Simplified circuit schematic of the ac-coupled bipolar pulse technique showing the three biases, digital bit code  $D$ , microwave with frequency  $f_m$ , and compensation AWG, applied to a single array of  $N$  Josephson junctions and its output voltage [12].

the pattern's sampling frequency  $f_s$  and the microwave signal with frequency  $f_m$ , are combined with a directional coupler (C), ac-coupled through an alternating series of two dc blocking capacitors (one shown) with 250 MHz cutoff frequency and three 1 dB attenuators (not shown) and applied via a semirigid coax and a normal-metal coplanar waveguide interface board to an  $N$  junction Josephson array (symbolically represented by  $X \cdot \cdot \cdot X$ ). The array used in this paper has  $N = 6400$  junctions, a minimum critical current of  $I_c = 7.2$  mA, and an average junction resistance  $R = 5.1$  m $\Omega$  and resides in the center conductor of a tapered superconducting coplanar waveguide that is terminated by a 22.4  $\Omega$  resistor [35]. Two pairs of low-speed taps, with inductive chokes made of resistively damped superconducting coils [34], are used for the output voltage ( $V_{out}$ ) and the compensation current ( $I_{AWG}$ ) leads. In this technique, a compensation signal is required to replace the fundamental signal removed by the dc blocks.

The next advancement for the JAWS was the development of a ternary pulse generator, manufactured by Sympuls (model BMG30G-64M), that resistively combines signals from two pulse drivers to make a "three-level" source with zero voltage and pulses of both polarities [22], [23], [25]. This instrument's pulse drivers are clocked at 30 gigabits per second (Gb/s), triple that of the previous instrumentation, providing a 30 Gb/s NRZ signal. However, the ACJVS arrays required higher amplitude current pulses than the drivers could directly produce; hence, the best performance was eventually achieved with external amplifiers having bandwidths up to 65 GHz. With this instrument, arrays of both 5280 and 6400 junctions each demonstrated 110 mV RMS voltage per array with 2.2 mA of dither dc current, which we define as the dc "operating margin" over which the voltage waveform remains perfectly quantized. This current range also represents the current that can be provided to an external load without additional compensation at the synthesized frequency from another bias source. This operating margin at 110 mV per array is comparable with that of the 125 mV waveform achieved on the same array with bipolar biasing with and without amplification, as shown in the first three data columns of Table I.

Investigations of waveforms synthesized with the Sympuls synthesizer and with amplifiers of different bandwidths demonstrated that the operating margins were still being limited by nonlinear response of both output drivers [23] and amplifiers. Amplifiers with the broadest bandwidths better preserved harmonic content of the pulse waveforms, but voltage levels still

TABLE I  
DC CURRENT RANGE OPERATING MARGINS FOR DIFFERENT PULSE-BIAS ELECTRONICS, AMPLIFIERS, AND OUTPUT VOLTAGES

RMS Voltage for 2 kHz Sine	Operating Margins for 2nd-order-modulator code			
	Agilent & no amp	Sympuls & 40 GHz amp	Sympuls & 65 GHz amp	HSCC & 40 GHz amp
110 mV ( $n=1$ )	-	1.9 mA	2.2 mA	-
125 mV ( $n=1$ )	1.8 mA	-	-	2.9 mA
250 mV ( $n=2$ )	0	0	0	0.9 mA

significantly varied with pulse density (typically referred to as "mark density") for both the driver and amplifier output signals. Even the unipolar output of a single output driver showed significant amplitude variation with pulse density in both the zero- and high-voltage levels. However, the larger output signals provided by the broadband amplifiers enabled, for the first time, operating margins of some waveforms on the second quantum state (i.e.,  $n = 2$ , in which each junction generates precisely two quantized pulses for every input pulse). However, quantization and practical operating margins were achieved only at lower voltages with pulse densities less than 50%.

In this paper, we present new bias electronics and two new bias techniques, which are the results of our efforts to improve the ACJVS operating margins of waveforms in the first quantum state and double the output voltage per array by achieving operating margins with the second quantum state. This improved ACJVS performance was accomplished by minimizing the junction response to the effects of the amplifier and output driver nonlinearities and, thus, their dependence on pulse density.

### III. NEW PULSE-BIAS ELECTRONICS

The new pulse-bias electronics (model ABG-2), custom designed by High Speed Circuit Consultants (HSCC) for this project, directly provides the pulse, microwave, and compensation signals required to bias two arrays. Integration of these three bias signals (required by this ac-coupled bipolar bias technique) into one instrument dramatically improves the phase stability of the microwave signal with respect to the pulse stream and also ensures that the compensation signal is synchronized with the pulse stream. The instrument uses a single microwave source that is tunable from  $f_m = 10$  to 15 GHz and can be phase-locked to an external 10 MHz frequency reference. A field-programmable gate array with 32 Gb of SDRAM for pattern storage provides the pulse-stream digital data to a 4:1 high-speed digital Multiplexer (MUX). This memory is adequate to synthesize 1 Hz waveforms. The MUX, which is specified to operate up to 28 Gb/s, produces an NRZ output at a bit rate corresponding to twice the microwave source frequency. The multiplexer used for the results in this paper was overclocked beyond its specification to 30 GHz with no degradation in performance. The amplitude and phase-adjusted microwave bias for each array is generated from the microwave source by a quadrature mixer. This bias is combined with the amplified pulse signal by a standard microwave coupler inside the instrument. The compensation bias is generated by two

DAC converters clocked at  $1/320$  of the microwave source frequency.

The advantages of having all three bias signals referenced to a common *microwave* clock are that it ensures continuous synchronization between those signals, simplifies system operation and automation, and allows day-to-day reproducibility of the relative phases of each bias. In the original bipolar pulse-bias systems, intermittent unlocking of the phase between these bias signals was a significant limitation because each bias was provided by separate commercial instruments that were frequency referenced to each other only through the 10 MHz instrument references. In these original systems, the internal frequency reference would periodically relock, thus changing that instrument's signal's phase relative to the other instruments and requiring realignment of the phase. Additionally, drifts of tens of picoseconds in the 10 MHz reference circuitry required correction by frequent adjustment of the microwave bias phase. This prevented continuous calibration and measurement; it also complicated system automation. The ABG-2 electronics, with fully integrated biases, allows intrinsic phase and frequency locking between all six bias signals sufficient for biasing two arrays and, thus, full system automation.

The ABG-2 electronics allowed the realization of two new bias techniques with a 15 GHz microwave frequency. The first of these newly realizable bias techniques is the ac-coupled bipolar bias technique with  $m = 1$ . With this condition, in which the microwave frequency is precisely half that of the NRZ clock frequency (two bits of the bitstream for each microwave period), the two-level ternary-coded signal and the microwave signal combine in such a way as to eliminate *all* pulses when representing the ZERO state of the ternary code. This particular feature is made possible by the 30 GHz NRZ clock of the new electronics, which is three times faster than the original bipolar electronics. The faster clock allows output drivers to generate 15 Gb/s RZ pulses that can be effectively canceled with the microwave signal using the appropriate relative phase.

#### IV. AC-COUPLED BIPOLAR PULSE-BIAS TECHNIQUE

In order to explain the  $m = 1$  state, we first review the original "bipolar" pulse phase-alignment scheme [4], [5], as shown in Fig. 2(a)–(c), where  $m = 3$ . This scheme was typically used in the original bipolar bias electronics, which used a 10 GHz NRZ clock [4], [5]. The desired output signal is first converted to a three-level digital code by use of a second-order delta-sigma modulator [36]. In our bipolar bias scheme, the ternary levels, namely, PLUS, MINUS, and ZERO, are then transformed into a two-level code, as shown in Fig. 2(a), by representing each ternary level as a unique pair of consecutive bits in the time domain 1 1,  $-1 -1$ , and  $-1 1$ . With proper phase alignment of the microwave signal, as shown in Fig. 2(b), the resulting combined digital and microwave signal, as shown in Fig. 2(c), produces precisely three positive-polarity pulses (representing PLUS), three negative-polarity pulses (representing MINUS), and a pair of negative- and positive-polarity pulses (representing ZERO) that produce zero *net* dc voltage.

The fourth bit pair 1  $-1$ , as shown in the last two NRZ periods in Fig. 2(a) (7 and 8), is inverted with respect to

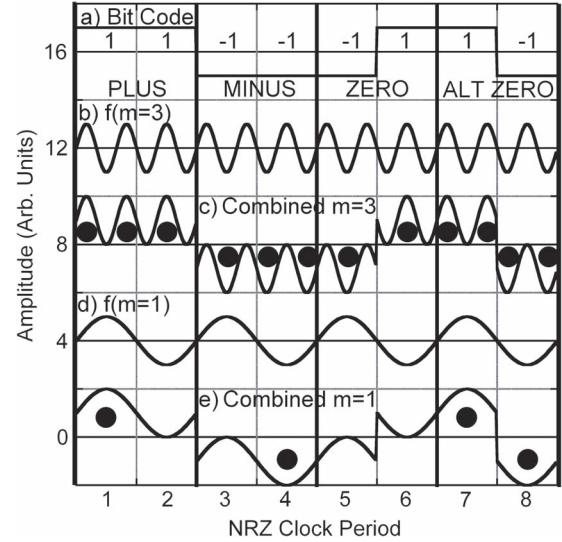


Fig. 2. Idealized bias waveforms for original [4], [5] and new bipolar bias schemes (waveforms are consecutively offset vertically from origin by 4 units). (a) Digital bit code signal showing four pairs of bits aligned to the NRZ clock  $f_s$ . (b) Microwave bias with  $f(m=3) = (3/2) f_s$ . (c) Combined original  $m = 3$  waveform where "correct" phase ZERO state has one pair of opposite polarity pulses. (d) Microwave bias with  $f(m=1) = (1/2) f_s$ . (e) Combined new  $m = 1$  waveform where "correct" phase ZERO state has no pulses. ZERO and ALT ZERO states (NRZ clock periods 5–8) are used for the zero-compensation bias technique. Filled circles indicate pulse locations.

the ZERO state; hence, it can also equivalently represent an alternate zero state (ALT ZERO) of the ternary representation. However, this phase alignment, which produces twice as many pulses as the  $-1 1$  bit pair, has been shown to yield smaller operating margins [5] due to the faster rise time of the combined waveform and the additional pulses. In order to maintain the largest operating margins, a custom modulator algorithm was created that excludes this pair from the transformed bit code. However, this alternate state can be still realized experimentally by shifting the microwave phase by  $180^\circ$ . Thus, ACJVS synthesizers using the bipolar bias technique must take care to avoid this "incorrect" ALT ZERO state and use the "correct" ZERO state.

#### V. IMPROVED PULSE-BIAS TECHNIQUE

The newly realizable bias technique with  $m = 1$  microwave frequency, as shown in Fig. 2(d), is combined with the digital bit code signal, as shown in Fig. 2(a), to produce the combined  $m = 1$  waveform shown in Fig. 2(e). This is the bipolar bias signal produced by the ABG-2 bitstream generator at maximum overclocked speed  $f_s = 30$  GHz and the same  $f_m = 15$  GHz microwave frequency as was used for the original Agilent electronics. The NRZ clock frequency for this case (30 GHz) is three times that used for the  $m = 3$  technique (10 GHz), whereas the microwave frequency was 15 GHz for both; hence, the pulse density and, thus, the maximum output voltage were the same. The ZERO state of the combined waveform over NRZ periods 5 and 6 shows that no Josephson pulses are generated. The no-pulse ZERO state for  $m = 1$  is ideal because it typically has larger margins than the other pulse states. In fact, earlier experiments and simulations of the Josephson junction dynamical response as a function of pulse spacing showed that

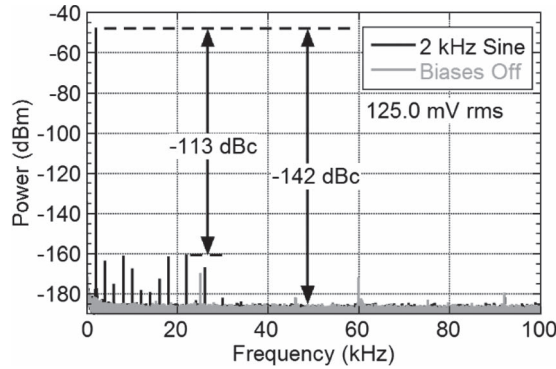


Fig. 3. Digitally sampled spectral measurement showing  $-113$  dBc [dB below the fundamental (carrier)] low-distortion measurement of the 2 kHz 125 mV RMS signal synthesized with one array of the ACJVS when biased at the first quantum state ( $n = 1$ ). The digitizer used 1 M $\Omega$  input impedance, the 2 V input range, 2 Hz resolution bandwidth, 10 averages, and a 500 kS/s sampling rate. Gray-shaded data show the digitizer  $-142$  dBc noise floor and spurious signals with the ACJVS pulses off.

the dc current range over which the junction locks to a pulse increases as the pulse density decreases [1], [5]. One way to look at these three states is that they are effectively realizing, within two NRZ periods, the same states produced by the  $n = +1, -1$ , and 0 Shapiro steps generated with the continuous-wave microwave bias signal.

The method to optimize the microwave and digital bias amplitudes is as follows. First, apply only the microwave bias and adjust the amplitude to maximize the dc current range of the  $n = 1$  Shapiro step. Next, apply the compensation bias, which is a sine wave at the desired signal frequency, and adjust its amplitude to switch between the two voltage steps produced by the  $n = +1$  and the  $n = -1$  Shapiro steps. Then, apply the digital bit code signal and adjust its amplitude and relative phase with respect to the microwave signal to maximize the dc current range of the quantized state produced with the combined waveform and the compensation. Depending on the junction dynamics (junction characteristics, microwave frequency, and power), the digital and microwave signals will not perfectly cancel in the ZERO state; however, the combined signal should be small enough that the junctions do not pulse for the ZERO state and pulse with appropriate polarity only for the PLUS and MINUS states as they are in the  $n = 1$  first quantum state.

Fig. 3 shows the measured spectrum of a 2 kHz sine wave synthesized with the ABG-2 electronics using the  $m = 1$  bipolar bias technique. The observed harmonics result from the nonlinearities of the analog-to-digital converter (ADC) that was used to acquire the spectra, as determined via a number of experimental methods such as modulating the biases and changing the ADC range and calibration. The bias amplitudes were adjusted to produce the  $n = 1$  quantum state, in which each junction produces precisely one pulse for every input pulse provided by the combined waveform. The amplitude of the digitally sampled waveform was defined to be 0.890509 of full scale to precisely produce 125.000 mV RMS for this 6400-junction array. The microwave power applied to the top of the cryoprobe at room temperature was  $+11.7$  dBm (dB with respect to 1 mW). As shown in the last column of Table I, the operating margins for this waveform are 2.9 mA, which is a

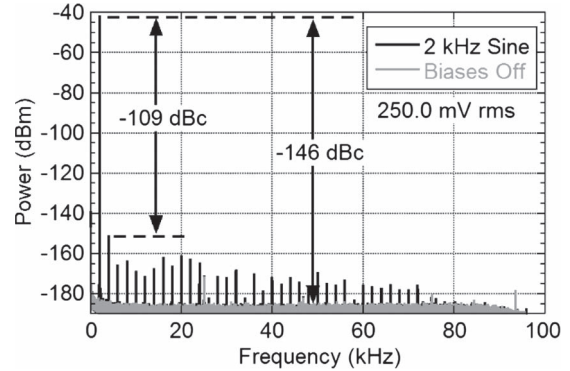


Fig. 4. Same measurement as Fig. 3, except that the voltage is doubled, because the array is biased at the second quantum state ( $n = 2$ ) and the sampling rate is 200 kS/s.

full milliampere larger than the 1.8 mA and 1.9 mA margins achieved with the same circuit using the  $m = 3$  original bias configurations with and without pulse amplification using the same array. This is a dramatic improvement in margins even over that achieved with the Sympuls electronics, whose margins are shown for a slightly lower 110 mV amplitude (that typically produces larger margins) and which also accesses three quantum states of the Josephson junctions with pulses of both polarity and no pulses.

The margins for the  $m = 1$  case are larger than those for the  $m = 3$  case because there are no pulses for the ZERO state. The time-dependent waveform of the bit code of the ZERO state has the most harmonic content and is the most challenging to produce by both output drivers (both Agilent and HSCC) and amplifiers. Thus, the ZERO states of the bit code are the most susceptible to distortion from nonlinearities. For the  $m = 3$  case, the resulting variations in the ZERO bit code result in pulse-amplitude variations that reduce the operating margins. However, for the  $m = 1$  case, the resulting imperfections in the digital waveform have little effect on the margins because there are no quantized pulses produced due to the approximate cancelation of the NRZ bitstream with the microwave signal in the combined waveform. The  $m = 1$  case effectively places the most problematic nonlinearity limitations of the high-speed bias electronics (drivers and amplifiers) to the state where the Josephson junctions have the best performance, i.e., producing zero pulses.

## VI. SECOND QUANTUM STATE

The dramatically larger operating margins achieved with the  $m = 1$  bipolar bias technique using the ABG-2 and higher output amplitudes available with amplification also allow, for the first time at maximum pulse density, realization of the  $n = 2$  second quantum state. Fig. 4 shows the measured spectrum of the same 2 kHz waveform synthesized with the ABG-2 electronics using the  $m = 1$  bipolar bias technique, such that the array produces precisely 250.000 mV RMS. As shown in Fig. 3, the observed harmonics result from the nonlinearities of the ADC that was used to measure the signal. The observed ADC distortion happens to be larger than was observed for the 275 mV waveform presented in [3] because the ADC had not been recently calibrated. The bias amplitudes were adjusted

to produce the  $n = 2$  second quantum state, in which each junction produces precisely two pulses for every input pulse provided by the combined waveform. For the  $n = 2$  Shapiro step, the microwave power applied to the top of the cryoprobe at room temperature was +13.0 dBm. As shown in the bottom cell of the last column of Table I, the operating margin for this waveform is 0.9 mA. This is the largest quantum-accurate ac voltage synthesized with a single array, and the operating margin is more than sufficient to perform ac voltage calibrations. Previously, this amplitude could be achieved only with the two-array ACJVS circuits. With both channels of the ABG-2 signals biasing a two-array ACJVS circuit, a quantum-accurate RMS voltage of 500 mV should be possible.

### VII. SYSTEMATIC ERRORS

While this first new bias technique yielded improved operating margins for the first quantum state and achieved a record of 250 mV RMS output voltage per array by enabling the  $n = 2$  quantum state, the second new bias technique addresses a difficulty in experimentally realizing accurate voltages at higher frequencies. The problem occurs at signal frequencies above 100 kHz, where inductance in the circuit between the output voltage taps can produce an undesired voltage signal  $V_L$  that is in quadrature with the desired synthesized signal. The inductance is primarily from the superconducting wiring between the Josephson junctions in the array, which is about 9 nH for our 6400-junction double-stacked array. A smaller 0.3 nH contribution is from the Josephson inductance that results from the kinetic inductance of the Josephson junctions, which scales in inverse proportion to the critical current. The largest signal that drives the inductance is the compensation bias. Smaller signals that may also contribute to the inductive voltage are any remaining “feedthrough” signals, most importantly at the fundamental, from the amplified digital bit code signal that are not sufficiently attenuated by the dc blocks. These signals are proportionally less attenuated at higher waveform frequencies. Another possible error contribution is input–output coupling  $V_{IO}$ , where signals couple to the output voltage leads from either the compensation bias or the feedthrough signals. These error signals were previously discussed [37]–[39], and they each become increasingly problematic for synthesized signals with frequencies greater than 100 kHz.

One previous approach to reducing this systematic error has been to synthesize small-amplitude waveforms, typically less than 10% of the  $n = 1$  Shapiro step voltage and up to 20% for some devices and bias conditions [20]. Since these small signals require equally small compensation signals, operating margins may be still obtained without compensation bias while still retaining the quantized state for the pulses. Unfortunately, the margins monotonically decrease as the waveform amplitude is increased. Eliminating the compensation thus eliminates the inductive error  $V_L$  from the compensation bias. A comparison between the output voltage from the circuit, if it is either compensation biased or unbiased, provides a method to characterize the magnitude and phase of  $V_L$ , which can then be used to bound or estimate the systematic error contribution of  $V_L$  in larger synthesized signals. Similarly, for larger signals,  $V_L$  may

be partially elucidated by changing the phase of the compensation signal. Both of these measurements may be required to evaluate this inductive-voltage systematic error for signals greater than 100 kHz.

### VIII. ZERO-COMPENSATION BIAS TECHNIQUE

The second new bias technique, which will be described below and we identify as the “zero-compensation” bias technique, may be a superior method to reduce this systematic error. It is valid to about 25% of the  $n = 1$  Shapiro step voltage. In this technique, the desired output signal is converted to a *two*-level digital code by use of a *first*-order delta–sigma modulator. Similar to the bipolar bias technique, the resulting *high* and *low* states are transformed into a two-level code that are each represented by a unique pair of consecutive bits in the time domain,  $-1$  and  $1$ , namely, the ZERO and ALT ZERO states shown in Fig. 2(e) as NRZ periods 5–8. Both states produce zero net pulses. However, if a dc bias is applied and the pulse density remains less than 50% such that each ALT ZERO state is always followed by at least one ZERO state, then the Josephson junctions will produce a unipolar single pulse for each ALT ZERO state. In terms of the washboard potential model that is an analog for describing the Josephson junction dynamics, the dc bias tilts the washboard, which results in  $2\pi$  change in phase for each ALT ZERO state.

As a result of the 50% maximum pulse density requirement, this technique produces unipolar pulses whose peak-to-peak amplitude is limited to half that of the  $n = 1$  Shapiro step voltage. The maximum amplitude with this bias technique is only 25% that of the bipolar bias technique and, likewise, only 25% of the  $n = 1$  Shapiro step voltage. Research to date on this bias technique also suggests that a first-order delta–sigma modulator is the most successful method in producing the largest amplitude waveforms, which is likely related to the pulse density requirement. Smaller amplitude waveforms can be synthesized with higher order modulators.

The main advantage of using this zero-compensation bias scheme with these two net-zero states is that the digital code has a much smaller fundamental signal. Fast Fourier transforms (FFTs) of the two-level (i.e., *high* and *low*) delta–sigma-modulated code (black) and its resulting dual-bit (ZERO and ALT ZERO) transformed code (gray) are shown in Fig. 5. The amplitude of the fundamental in the transformed code is reduced by 134 dB for this 2 kHz waveform, which has an amplitude that is 0.249343 fraction of full scale. Note that a negative dc offset of 0.2499849 full scale is also included in the waveform so that the peak voltage does not exceed 50% full scale, thus ensuring that there are no consecutive pulses. Including the dc offset in the synthesized waveform ensures that the voltage remains between 0 V and half the  $n = 1$  Shapiro step voltage. Applying the zero-compensation bias technique to the 6400-junction array, this 2 kHz digital code produces an ac RMS voltage of precisely 35.0000 mV with a 49.6 mV dc offset, with an operating margin of 2.9 mA.

A 1 MHz waveform, with the same 35 mV RMS ac amplitude and 49.6 mV dc offset as the 2 kHz waveform, was also synthesized with the zero-compensation bias technique and achieved

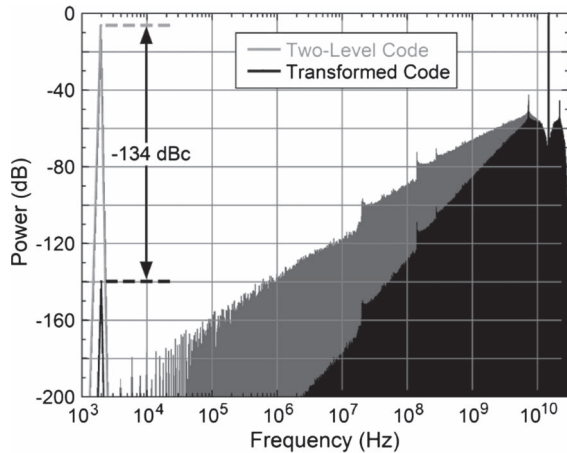


Fig. 5. Calculated spectra of the FFT of the two-level digital code sequence (gray) and its transformed code (black) for a 2 kHz signal. The transformed code, which is used in the zero-compensation bias technique, converts the two levels to the ZERO and ALT ZERO states [see Fig. 2(e)] with zero-net pulses for each bit pair, resulting in a fundamental amplitude reduced by 134 dB.

an operating margin of 2.8 mA. The microwave power applied to the top of the cryoprobe at room temperature was +5.5 dBm. Fig. 6 shows the measured FFT of this waveform. Comparing the FFTs of the 1 MHz digital codes (neither are shown), the 1 MHz amplitude is reduced by 80 dB for the transformed code compared with that of the two-level delta-sigma-modulated code. This reduction is much less than that achieved for the 2 kHz pattern in Fig. 5 because of the response of the first-order modulator. Nevertheless, the reduced fundamental of the digital code is significant, and we further experimentally reduced its amplitude and those of the other feedthrough signals with the series of dc blocks and attenuators. The remaining unblocked feedthrough signals that are produced by the bit code, as well as from distortion generated by the pulse output driver and the amplifier, will still bias the array inductance and may or may not also appear in the output waveform (from input-output coupling). The presence of these signals can be measured by turning off the microwave and compensation signals provided that the junctions remain in the zero quantum state and are not pulsing. The resulting “Feedthrough” signals are shown in Fig. 6 as the light gray measured data. The harmonics are more than 90 dB below the amplitude of the synthesized 1 MHz tone; thus, they will not contribute to the total RMS voltage. However, the  $-98$  dBc feedthrough signal at 1 MHz, which is a combination of input-output  $V_{IO}$  or inductive  $V_L$  error signals, will certainly contribute because this signal adds vectorially to the synthesized signal at a part in  $10^5$  in voltage (or less) depending on the relative phases. As aforementioned and in previous papers describing the systematic errors associated with such signals, there are various methods to measure and then to reduce, bound, or calibrate such systematic errors [37]–[39].

In summary of the zero-compensation bias technique, operating margins greater than 2.8 mA were demonstrated for both 2 kHz and 1 MHz waveforms. Thus, the zero-compensation bias technique provides a new method to synthesize arbitrary waveforms with significant operating margins that eliminate inductive voltage errors due to compensation bias. Two drawbacks of this technique are that a dc bias is required and the

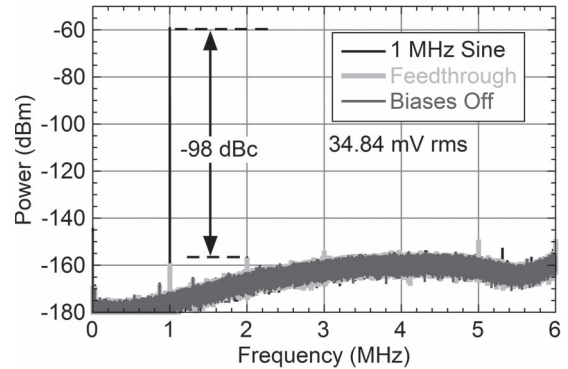


Fig. 6. Digitally sampled spectral measurement of a 1 MHz 34.84 mV RMS signal synthesized with one array of the ACJVS with the “zero-compensation” bias technique, when biased at the first quantum state ( $n = 1$ ). The digitizer used 1 M $\Omega$  input impedance, 2 V input range, 100 Hz resolution bandwidth, 10 averages, and 15 MS/s sampling rate. Dark-gray-shaded data show the digitizer noise floor. Light gray data show the inductive voltage signal from the remaining feedthrough digital signal.

peak amplitude that can be synthesized is one-fourth that of the  $n = 1$  Shapiro step voltage. A more challenging drawback is the inherent dc offset of the output waveform, which prevents the practical implementation of RMS measurements. However, we note that this offset can be eliminated by either ac-coupling the output or by use of a series-connected second array that produces the same ac waveform (and phase) but has the opposite polarity dc voltage.

## IX. CONCLUSION

In conclusion, we have developed new bias electronics in which all three biases required to operate a single array of a JAWS circuit are fully integrated into a single instrument with a common clock. We have demonstrated the  $m = 1$  bipolar bias technique with improved operating margins for waveforms synthesized in the first quantum state, and we have demonstrated operating margins in the second quantum state with a record of 250 mV RMS voltage. We have also demonstrated a new zero-compensation bias technique that achieves operating margins without a compensation bias signal at the synthesized frequency. This zero-compensation bias technique may be particularly useful to synthesize waveforms with frequencies greater than 100 kHz, where systematic errors from circuit inductances and from input-output coupling can compromise realization of the intrinsic accuracy expected from waveforms synthesized with the perfectly quantized pulses produced by arrays of Josephson junctions.

## ACKNOWLEDGMENT

The authors would like to thank P. D. Dresselhaus for many years of collaboration and assistance in developing the pulse-drive instrumentation.

## REFERENCES

- [1] S. P. Benz and C. A. Hamilton, “A pulse-driven programmable Josephson voltage standard,” *Appl. Phys. Lett.*, vol. 68, no. 22, pp. 3171–3173, May 27, 1996.
- [2] T. E. Lipe *et al.*, “Thermal voltage converter calibrations using a quantum AC standard,” *Metrologia*, vol. 45, no. 3, pp. 275–280, Jun. 2008.

- [3] S. P. Benz *et al.*, "Progress toward a 1 V pulse-driven AC Josephson voltage standard," *IEEE Trans. Instrum. Meas.*, vol. 58, no. 4, pp. 838–843, Apr. 2009.
- [4] S. P. Benz, C. A. Hamilton, C. J. Burroughs, and T. E. Harvey, "AC and DC bipolar voltage source using quantized pulses," *IEEE Trans. Instrum. Meas.*, vol. 48, no. 2, pp. 266–269, Apr. 1999.
- [5] S. P. Benz, C. J. Burroughs, T. E. Harvey, and C. A. Hamilton, "Operating conditions for a pulse-quantized AC and DC bipolar voltage source," *IEEE Trans. Appl. Supercond.*, vol. 9, no. 2, pp. 3306–3309, Jun. 1999.
- [6] S. P. Benz, C. J. Burroughs, P. D. Dresselhaus, and L. A. Christian, "AC and DC voltages from a Josephson arbitrary waveform synthesizer," *IEEE Trans. Instrum. Meas.*, vol. 50, no. 2, pp. 181–184, Apr. 2001.
- [7] C. J. Burroughs, S. P. Benz, P. D. Dresselhaus, and Y. Chong, "Precision measurements of AC Josephson voltage standard operating margins," *IEEE Trans. Instrum. Meas.*, vol. 54, no. 2, pp. 624–627, Apr. 2005.
- [8] B. Jeanneret and S. P. Benz, "Application of the Josephson effect in electrical metrology," *Eur. Phys. J. Spec. Topics*, vol. 172, no. 1, pp. 181–206, Jun. 2009.
- [9] S. P. Benz, "Synthesizing accurate voltages with superconducting quantum-based standards," *IEEE Instrum. Meas. Mag.*, vol. 13, no. 3, pp. 8–13, Jun. 2010.
- [10] N. H. Kaneko, M. Maruyama, and C. Urano, "Current status of Josephson arbitrary waveform synthesis at NMIJ/AIST," *IEICE Trans. Electron.*, vol. E94-C, no. 3, pp. 273–279, Mar. 2011.
- [11] S. P. Benz, C. J. Burroughs, and P. D. Dresselhaus, "Low harmonic distortion in a Josephson arbitrary waveform synthesizer," *Appl. Phys. Lett.*, vol. 77, no. 7, pp. 1014–1016, Aug. 2000.
- [12] S. P. Benz, C. J. Burroughs, and P. D. Dresselhaus, "AC coupling technique for Josephson waveform synthesis," *IEEE Trans. Appl. Supercond.*, vol. 11, no. 1, pp. 612–616, Mar. 2001.
- [13] S. P. Benz, P. D. Dresselhaus, J. Martinis, and S. W. Nam, "An AC Josephson source for Johnson noise thermometry," *IEEE Trans. Instrum. Meas.*, vol. 52, no. 2, pp. 545–549, Apr. 2003.
- [14] J. M. Williams *et al.*, "The simulation and measurement of the response of Josephson junctions to optoelectronically generated short pulses," *Supercond. Sci. Technol.*, vol. 17, no. 6, pp. 815–818, Jun. 2004.
- [15] O. A. Chevtchenko *et al.*, "Realization of a quantum standard for AC voltage: Overview of a European research project," *IEEE Trans. Instrum. Meas.*, vol. 54, no. 2, pp. 628–631, Apr. 2005.
- [16] S. P. Benz, C. J. Burroughs, P. D. Dresselhaus, T. E. Lipe, and J. R. Kinard, "100 mV AC–DC transfer standard measurements with a pulse-driven AC Josephson voltage standard," in *Proc. 25th CPEM*, 2006, pp. 678–679.
- [17] S. P. Benz *et al.*, "An AC Josephson voltage standard for AC–DC transfer standard measurements," *IEEE Trans. Instrum. Meas.*, vol. 56, no. 2, pp. 239–243, Apr. 2007.
- [18] C. Urano *et al.*, "Observation of quantized voltage steps using a Josephson junction array driven by optoelectronically generated pulses," *IEEE Trans. Instrum. Meas.*, vol. 56, no. 2, pp. 614–618, Apr. 2007.
- [19] O. F. Kieler *et al.*, "SNS Josephson junction series arrays for the Josephson arbitrary waveform synthesizer," *IEEE Trans. Appl. Supercond.*, vol. 17, no. 2, pp. 187–190, Jun. 2007.
- [20] S. P. Benz, P. D. Dresselhaus, C. J. Burroughs, and N. F. Bergren, "Precision measurements using a 300 mV Josephson arbitrary waveform synthesizer," *IEEE Trans. Appl. Supercond.*, vol. 17, no. 2, pp. 864–869, Jun. 2007.
- [21] O. F. O. Kieler, R. P. Landim, S. P. Benz, P. D. Dresselhaus, and C. J. Burroughs, "AC–DC transfer standard measurements and generalized compensation with the AC Josephson voltage standard," *IEEE Trans. Instrum. Meas.*, vol. 57, no. 4, pp. 791–796, Apr. 2008.
- [22] H. E. van den Brom, E. Houtzager, B. E. R. Brinkmeier, and O. A. Chevtchenko, "Bipolar pulse-drive electronics for a Josephson arbitrary waveform synthesizer," *IEEE Trans. Instrum. Meas.*, vol. 57, no. 2, pp. 428–431, Feb. 2008.
- [23] E. Houtzager, S. P. Benz, and H. E. van den Brom, "Operating margins for a pulse-driven Josephson arbitrary waveform synthesizer using a ternary bit-stream generator," *IEEE Trans. Instrum. Meas.*, vol. 58, no. 4, pp. 775–780, Apr. 2009.
- [24] R. C. Toonen and S. P. Benz, "Nonlinear behavior of electronic components characterized with precision multitones from a Josephson arbitrary waveform synthesizer," *IEEE Trans. Appl. Supercond.*, vol. 19, no. 3, pp. 715–718, Jun. 2009.
- [25] E. Houtzager, H. E. van den Brom, and D. van Woerkom, "Automatic tuning of the pulse-driven AC Josephson voltage standard," in *Proc. 27th CPEM*, 2010, pp. 185–186.
- [26] S. P. Benz, P. D. Dresselhaus, and C. J. Burroughs, "Multitone waveform synthesis with a quantum voltage noise source," *IEEE Trans. Appl. Supercond.*, vol. 21, no. 3, pp. 681–686, Jun. 2011.
- [27] T. Hagen, I. Budovsky, S. P. Benz, and C. J. Burroughs, "Calibration system for AC measurement standards using a pulse-driven Josephson voltage standard and an inductive voltage divider," in *Proc. 28th CPEM*, 2012, pp. 672–673.
- [28] C. J. Burroughs, S. P. Benz, P. D. Dresselhaus, Y. Chong, and H. Yamamori, "Flexible cryo-packages for Josephson devices," *IEEE Trans. Appl. Supercond.*, vol. 15, no. 2, pp. 465–468, Jun. 2005.
- [29] P. D. Dresselhaus, Y. Chong, and S. P. Benz, "Stacked Nb–MoSi<sub>2</sub>–Nb Josephson junctions for AC voltage standards," *IEEE Trans. Appl. Supercond.*, vol. 15, no. 2, pp. 449–452, Jun. 2005.
- [30] N. Hadacek, P. D. Dresselhaus, and S. P. Benz, "Lumped 50-Ω arrays of SNS Josephson junctions," *IEEE Trans. Appl. Supercond.*, vol. 16, no. 4, pp. 2005–2010, Dec. 2006.
- [31] M. Schubert, T. May, G. Wende, and H.-G. Meyer, "A cross-type SNS junction array for a quantum-based arbitrary waveform synthesizer," *IEEE Trans. Appl. Supercond.*, vol. 15, no. 2, pp. 829–832, Jun. 2005.
- [32] Y. Chong *et al.*, "Josephson junctions with nearly superconducting metal silicide barriers," *Appl. Phys. Lett.*, vol. 87, no. 22, pp. 222511-1–222511-3, Nov. 2005.
- [33] B. Baek, P. D. Dresselhaus, and S. P. Benz, "Co-sputtered amorphous Nb<sub>x</sub>Si<sub>1-x</sub> barriers for Josephson-junction circuits," *IEEE Trans. Appl. Supercond.*, vol. 16, no. 4, pp. 1966–1970, Dec. 2006.
- [34] M. Watanabe, P. D. Dresselhaus, and S. P. Benz, "Resonance-free low-pass filters for the AC Josephson voltage standard," *IEEE Trans. Appl. Supercond.*, vol. 16, no. 1, pp. 49–53, Mar. 2006.
- [35] P. D. Dresselhaus, M. M. Elsbury, and S. P. Benz, "Tapered transmission lines with dissipative junctions," *IEEE Trans. Appl. Supercond.*, vol. 19, no. 3, pp. 993–998, Jun. 2009.
- [36] J. C. Candy, "An overview of basic concepts," in *Delta-Sigma Data Converters: Theory, Design, Simulation*, S. R. Norsworthy, R. Schreier, and G. C. Temes, Eds. Piscataway, NJ, USA: IEEE Press, 1997.
- [37] C. J. Burroughs, S. P. Benz, and P. D. Dresselhaus, "AC Josephson voltage standard error measurements and analysis," *IEEE Trans. Instrum. Meas.*, vol. 52, no. 2, pp. 542–544, Apr. 2003.
- [38] R. P. Landim, S. P. Benz, P. D. Dresselhaus, and C. J. Burroughs, "Systematic-error signals in the AC Josephson voltage standard: Measurement and reduction," *IEEE Trans. Instrum. Meas.*, vol. 57, no. 6, pp. 1215–1220, Jun. 2008.
- [39] P. S. Filipowski, J. R. Kinard, T. E. Lipe, Y. Tang, and S. P. Benz, "Correction of systematic errors due to the voltage leads in AC Josephson voltage standard," *IEEE Trans. Instrum. Meas.*, vol. 58, no. 4, pp. 853–858, Apr. 2009.

**Samuel P. Benz** (M'01–SM'01–F'10) was born in Dubuque, IA, USA, on December 4, 1962. He received the B.A. degree (*summa cum laude*) in physics and math from Luther College, Decorah, IA, in 1985 and the M.A. and Ph.D. degrees in physics from Harvard University, Cambridge, MA, USA, in 1987 and 1990, respectively. He was awarded an R.J. McElroy Fellowship (1985–1988) to work toward the Ph.D. degree.

In 1990, he joined the National Institute of Standards and Technology (NIST), Boulder, CO, USA, as a NIST/National Research Council Postdoctoral Fellow and became a permanent Staff Member in January 1992. He has been the Project Leader of the Quantum Voltage Project at NIST since October 1999. He has more than 160 publications and is the holder of three patents in the field of superconducting electronics. He has worked on a broad range of topics within the field of superconducting electronics, including Josephson junction array oscillators, single flux quantum logic, ac and dc Josephson voltage standards, Josephson waveform synthesis, and noise thermometry.

Dr. Benz is a Fellow of the American Physical Society and a member of Phi Beta Kappa and Sigma Pi Sigma. He was a recipient of three U.S. Department of Commerce Gold Medals for Distinguished Achievement and the 2006 IEEE Council on Superconductivity Van Duzer Prize.

**Steven B. Waltman** (M'88) was born in Fort Belvoir, VA, USA, on November 26, 1964. He received the B.S. degree in electrical engineering from California Institute of Technology, Pasadena, CA, USA, in 1988.

From 1986 to 1990, he developed a new class of sensors based on electron tunneling at the Jet Propulsion Laboratory, NASA. Since 1990, he has been with the Time and Frequency Division, National Institute of Standards and Technology, Boulder, CO, USA, as a Staff Physicist where he worked on optical frequency metrology technology. In 1998, he cofounded Geocast Network Systems, the first of several startup companies. He is currently the Proprietor of High Speed Circuit Consultants, Boulder, which is a company that provides custom electronics for quantum physics research. He has more than 20 publications and has 15 U.S. patents.